Inorg. Chem. **2004**, *43*, 1784–1792

Sensitization and Stabilization of TiO_2 Photoanodes with Electropolymerized Overlayer Films of Ruthenium and Zinc Polypyridyl Complexes: A Stable Aqueous Photoelectrochemical Cell

John A. Moss,[†] John C. Yang,[†] Jeremy M. Stipkala,[‡] Xingu Wen,[†] Carlo A. Bignozzi,[§] Gerald J. Meyer,[‡] and Thomas J. Meyer*[,†]

Department of Chemistry, University of North Carolina at Chapel Hill, Chapel Hill, North Carolina 27599-3290, Department of Chemistry, Johns Hopkins University, Baltimore, Maryland 21218, Dipartimento di Cimica dell'Universita, Centro di Studio su Fotoreattivita e Catalisi CNR, 44100 Ferrara, Italy

Received February 28, 2003

Overlayer thin films of vinylbipyridine (vbpy)-containing Ru and Zn complexes have been formed on top of ruthenium dye complexes adsorbed to TiO_2 by reductive electropolymerization. The goal was to create an efficient, water-stable photoelectrode or electrodes. An adsorbed-$[Ru(vbpy)_2(dcb)](PF_6)_2$/poly-$[Ru(vbpy)_3](PF_6)_2$ surface composite displays excellent stability toward dissolution in water, but the added overlayer film greatly decreases incident photon-to-current conversion efficiencies (IPCE) in propylene carbonate with I_3^-/I^- as the carrier couple. An ads-$[Ru(vbpy)_2(dcb)](PF_6)_2$/poly-$[Zn(vbpy)_3](PF_6)_2$ composite displays no loss in IPCE compared to ads-$[Ru(vbpy)_2(dcb)](PF_6)_2$ but is susceptible to film breakdown in the presence of water by solvolysis and loss of the cross-linking Zn^{2+} ions. Success was attained with an ads-$[Ru(vbpy)_2(dcb)](PF_6)_2$/poly-$[Ru(vbpy)_2(dppe)](PF_6)_2$ composite. In this case the electropolymerized layer is transparent in the visible. The composite electrode is stable in water, the IPCE in propylene carbonate with I_3^-/I^- is comparable to the adsorbed complex, and a significant IPCE is observed in water with the quinone/hydroquinone carrier couple. The assembly $[(bpy)_2(CN)Ru(CN)Ru(vbpy)_2(NC)Ru(CN)(bpy)_2](PF_6)_2$ ($[Ru(CN)Ru(NC)Ru](PF_6)_2$) adsorbs spontaneously on TiO_2, and electropolymerization of thin layers of the assembly to give ads-$[Ru(CN)Ru(NC)Ru](PF_6)_2$/poly-$[Ru(CN)Ru(NC)Ru](PF_6)_2$ enhances IPCE and has no deleterious effect on the IPCE/Ru.

Introduction

Much interest has been focused on photoelectrochemical cells utilizing dye-sensitized nanocrystalline TiO_2 electrodes since early reports of high photocurrent efficiencies. These cells consist of thin films of TiO_2 derivatized by adsorbed chromophores such as $[Ru(dcb)_3]^{2+}$ (dcb is 2,2′-bipyridine-4,4′-dicarboxylic acid) in a thin-layer arrangement of the TiO_2 anode and a platinum cathode with propylene carbonate containing I_3^-/I^- as an electron donor and electrolyte.[1−5] Since these initial investigations, the repertoire of molecular chromophores that efficiently sensitize colloidal semiconductor thin films has been extended.[6] The adsorbed assembly $[(bpy)_2(CN)Ru(CN)Ru(dcb)_2(NC)Ru(CN)(bpy)_2]^{2+}$ converts light to electricity with incident photon-to-current efficiency (IPCE) values in excess of 80% in a similar cell. With cells of this type, notable advances have been made in

* To whom correspondence should be addressed. Present address: Associate Director for Strategic Research, Los Alamos National Laboratory, P.O. Box 1663, MS A127, Los Alamos, NM 87545. E-mail: tjmeyer@lanl.gov.
[†] University of North Carolina at Chapel Hill.
[‡] Johns Hopkins University.
[§] Dipartimento di Cimica dell'Universita.

(1) Dabestani, R.; Bard, A. J.; Campion, A.; Fox, M. A.; Mallouk, T. E.; Webber, S. E.; White, J. M. *J. Phys. Chem.* **1988**, *92*, 1872.
(2) Meyer, G. J.; Pfennig, B. W.; Schoonover, J. R.; Timpson, C. J.; Wall, J. F.; Kobusch, C.; Chen, X.; Peek, B. M.; Wall, C. G.; Ou, W.; Erickson, B. W.; Bignozzi, C. A.; Meyer, T. J. *Inorg. Chem.* **1994**, *33*, 3952.
(3) O'Regan, B.; Grätzel, M. *Nature* **1991**, *353*, 737.
(4) Nazeeruddin, M. K.; Kay, A.; Rodicio, I.; Humphry-Baker, R.; Muller, P.; Liska, N.; Vlachopoulos, N.; Grätzel, M. *J. Am. Chem. Soc.* **1993**, *115*, 6382.
(5) Stanley, A.; Matthews, D. *Aust. J. Chem.* **1995**, *48*, 1293.
(6) (a) Argazzi, R.; Bignozzi, C. A.; Hasselmann, G. M.; Meyer, G. J. *Inorg. Chem.* **1998**, *37*, 4533. (b) Takahashi, Y.; Arakawa, H.; Sugihara, H.; Hara, K.; Islam, A.; Katoh, R.; Tachibana, Y.; Yanagida, M. *Inorg. Chim. Acta* **2000**, *310*, 169. (c) Nazeeruddin, M. K.; Pechy, P.; Renouard, T.; Zakeeruddin, S. M.; Humphry-Baker, R.; Comte, P.; Liska, P.; Cevey, L.; Costa, E.; Shklover, V.; Spiccia, L.; Deacon, G. B.; Bignozzi, C. A.; Grätzel, M. *J. Am. Chem. Soc.* **2001**, *123*, 1613.

10.1021/ic030081a CCC: $27.50
Published on Web 02/11/2004

understanding the processes of charge injection,[7] charge transport,[8] charge recombination,[9,10] and sensitizer regeneration.[11]

The highly efficient cells formed in this way exhibit excellent long-term stability in nonaqueous solvents, but the carboxylate complexes desorb from TiO_2 in the presence of even small amounts of water. Additionally, the maximum available cell potential is limited by the difference in potentials between the conduction band and the solution I_3^-/I^- couple. In propylene carbonate and other nonaqueous solvents, the redox couples available to serve the role of electron-transfer donor/redox carrier is somewhat limited, and it would be advantageous to explore an extended range of redox couples in water as the solvent. Phosphonate-derivatized chromophores have been used to stabilize surface structures in aqueous environments, but this approach is limited to acidic solutions.[12−16]

A potentially more versatile approach to stabilized surface structures is available by forming electropolymerized thin films of the dye on the semiconductor surface.[17] This article describes the evolution and exploitation of a successful strategy for forming surface-stabilized TiO_2 photoanodes on by electropolymerization. They are prepared by initial adsorption of the metal complex dye $[Ru(vbpy)_2(dcb)]^{2+}$ (**1**) (vbpy is 4-methyl-4′-vinyl-2,2′-bipyridine). This complex has both carboxylic acid functionalities for surface adsorption and polymerizable vinyl groups which can engage in reductive electropolymerization with vinyl-containing complexes in the external solution. Adsorption followed by electropolymerization creates thin copolymeric layers containing an adsorbed complex inside and an electropolymerized complex on the outside.

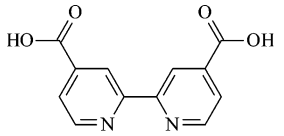

2,2'-bipyridine-4,4'-dicarboxylic acid (dcb)

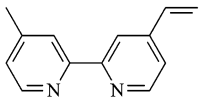

4-methyl-4'-vinyl-2,2'-bipyridine (vbpy)

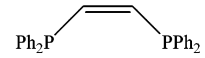

cis-1,2-bis(diphenylphosphino)-ethylene

This strategy has been pursued through three stages with the third successfully leading to water-stable surface structures with relatively high photocurrents. The three stages were based on overlayers of (1) poly-$[Ru(vbpy)_3](PF_6)_2$, which provides aqueous stability but low photocurrents because of competitive light absorption and quenching, (2) poly-$[Zn(vbpy)_3](PF_6)_2$, which is optically transparent in the visible and has high photocurrents but is unstable in water, and (3) poly-$[Ru(vbpy)_2(dppe)]^{2+}$, which is transparent in the low energy visible, has high photocurrents, and is water stable.

The cyano-bridged complex $[(bpy)_2(CN)Ru(CN)Ru(vbpy)_2(NC)Ru(CN)(bpy)_2]^{2+}$ (**2**) ($Ru(CN)Ru(CN)Ru^{2+}$) adsorbs to TiO_2 spontaneously, which provides a second approach to the formation of copolymeric layers by adsorption followed by electropolymerization. The resulting multilayer films sensitize TiO_2 and remain absorbed over a wide range of aqueous conditions. A preliminary account of this work has appeared elsewhere.[18]

Experimental Section

Materials. For electrochemical experiments, acetonitrile (Burdick and Jackson, spectrophotometric grade) or propylene carbonate (Aldrich) was deaerated by bubbling with N_2 and stored in an inert-atmosphere glovebox. Water was distilled and deionized with a Barnstead Nanopure System. Tin(IV)-doped indium oxide (ITO) electrodes were obtained from either Delta Technologies (20 Ω/□) or Libby Owens Ford (10 Ω/□) and were cleaned by sonicating 15 min in 1:1:5 $NH_4OH-H_2O_2-H_2O$ and rinsing with water and ethanol. Nanocrystalline TiO_2 electrodes were prepared by the method of Grätzel.[3] A literature procedure for the preparation of tetra-*n*-butylammonium hexafluorophosphate (TBAH) was used.[19] All other chemicals were reagent grade and used as received. The ligands 4-methyl-4′-vinyl-2,2′-bipyridine (vbpy),[19] 2,2′-bipyridyl-4,4′-dicarboxylic acid (dcb),[20] and 4,4′-biscarboxyethyl-2,2′-bipyridine $[(EtCO_2)_2bpy]$[21] were prepared according to literature procedures. The complexes $Ru(vbpy)_2Cl_2\cdot 2H_2O$,[19] $[Ru(vbpy)_3]$-

(7) Tachibana, Y.; Moser, J. E.; Grätzel, M.; Klug, D. R.; Durrant, J. *J. Phys. Chem.* **1996**, *100*, 20056. (b) Hannappel, T.; Burfeindt, B.; Storck, W.; Willig, F. *J. Phys. Chem. B* **1997**, *101*, 6799. (c) Heimer, T. A.; Heilweil, E. J. *J. Phys. Chem. B* **1997**, *101*, 10990. (d) Ellingson, R. J.; Asbury, J. B.; Ferrere, S.; Ghosh, H. N.; Sprague, J. R.; Lian, T.; Nozik, A. J. *J. Phys. Chem. B* **1997**, *101*, 6455. (e) Benko, G.; Kallioinen, J. E.; Korppi-Tommola, J. E. I.; Yartsev, A. P.; Sundstrom, V. *J. Am. Chem. Soc.* **2002**, *124*, 489.
(8) (a) Solbrand, A.; Lindstrom, H.; Rensmo, H.; Hagfeldt, A.; Lindquist, S.-E. *J. Phys. Chem B* **1997**, *101*, 2514. (b) Cao, F.; Oskam, G.; Searson, P. C.; Meyer, G. J. *J. Phys. Chem.* **1996**, *100*, 17021. (c) Konenkamp, R.; Henninger, R.; Hoyer, P. *J. Phys. Chem.* **1993**, *97*, 7328. (d) Schwarzburg, K.; Willig, F. *Appl. Phys. Lett.* **1991**, *58*, 2520.
(9) (a) Hasslemann, G. M.; Meyer, G. J. *J. Phys. Chem. B* **1999**, *103*, 7671. (b) Nelson, J. *Phys. Rev. B* **1999**, *59*, 15374. (c) Nelson, J.; Haque, S. A.; Klug, D. R.; Durrant, J. R. *Phys. Rev. B* **2001**, *63*, 205321.
(10) Moser, J. E.; Gratzel, M. *Chem. Phys.* **1993**, *176*, 493. (b) Lu, H.; Prieskorn, J. N.; Hupp, J. T. *J. Am. Chem. Soc.* **1993**, *115*, 4927. (c) Martini, I.; Hodak, J. H.; Hartland, G. V. *J. Phys. Chem. B.* **1998**, *102*, 607. (d) Martini, I.; Hodak, J. H.; Hartland, G. V. *J. Phys. Chem. B.* **1998**, *102*, 9508.
(11) (a) Nasr, C.; Hotchandani, S.; Kamat, P. V. *J. Phys. Chem. B* **1998**, *102*, 4944. (b) Pelet, S.; Moser, J.-E.; Grätzel, M. *J. Phys. Chem. B* **2000**, *104*, 1791.
(12) Zakeeruddin, S. M.; Nazeeruddin, M. K.; Pechy, P.; Rotzinger, F. P.; Humphry-Baker, R.; Kalyanasundaram, K.; Grätzel, M.; Shklover, V.; Haibach, T. *Inorg. Chem.* **1997**, *36*, 5937.
(13) Goff, A. H.; Joiret, S.; Falaras, P. *J. Phys. Chem. B* **1999**, *103*, 9569.
(14) Zaban, A.; Ferrere, S.; Sprague, J.; Gregg, B. A. *J. Phys. Chem. B* **1997**, *101*, 55.
(15) Yan, S. G.; Hupp, J. T. *J. Phys. Chem.* **1996**, *100*, 6867.
(16) Trammell, S. A.; Moss, J. A.; Yang, J.; Nakhle, B. M.; Slate, C. A.; Odobel, F.; Sykora, M.; Erickson, B. W.; Meyer, T. J. *Inorg. Chem.* **1999**, *38*, 3665.
(17) Abrũna, H. D.; Denisevich, P.; Umana, M.; Meyer, T. J.; Murray, R. W. *J. Am. Chem. Soc.* **1981**, *103*, 1.
(18) Moss, J. A.; Stipkala, J. M.; Yang, J. C.; Bignozzi, C. A.; Meyer, G. J.; Meyer, T. J.; Wen, X.; Linton, R. W. *Chem. Mater.* **1998**, *10*, 1748.
(19) Leasure, R. M.; Ou, W.; Moss, J. A.; Linton, R. W.; Meyer, T. J. *Chem. Mater.* **1996**, *8*, 264.
(20) Launikonis, A.; Lay, P. A.; Mau, A. W. H.; Sargeson, A. M.; Sasse, W. H. F. *Aust. J. Chem.* **1986**, *39*, 1053.
(21) Anderson, P. A.; Deacon, G. B.; Haarmann, K. H.; Keene, F. R.; Meyer, T. J.; Reitsma, D. A.; Skelton, B. W.; Strouse, G. F.; Thomas, N. C.; Treadway, J. A.; White, A. H. *Inorg. Chem.* **1995**, *34*, 6145.

$(PF_6)_2$,[17] $[Zn(vbpy)_3](PF_6)_2$,[22] and $[(bpy)_2(CN)Ru(CN)Ru(vbpy)_2(NC)Ru(CN)(bpy)_2](PF_6)_2$[23] were prepared as previously reported.

Preparation of $[Ru(vbpy)_2(dcb)](PF_6)_2$. The synthesis of $[Ru(vbpy)_2(dcb)](PF_6)_2$ was carried out by using a modification of the literature preparation of the complexes of the type $[Ru(bpy)_2(LL)]^{2+}$ (LL is a bidentate phosphine or arsine ligand).[24] In a typical preparation, $Ru(vbpy)_2Cl_2 \cdot 2H_2O$ (1 equiv) and $(EtCO_2)_2bpy$ (2.5 equiv) were dissolved in 2:1 $CH_3CH_2OH-H_2O$ which had been deaerated by sparging with Ar. The solution was heated at reflux for 4 h, with the color changing from purple to red/orange over the course of the reaction. The reaction mixture was cooled, and the ethanol was removed by rotary evaporation. The aqueous reaction mixture was diluted to 1.5 L with water and loaded onto a SP Sephadex C-25 column (15 in. × 1 in.). The $[Ru(vbpy)_2((EtCO_2)_2bpy)](NO_3)_2$ product was removed by elution with 0.15 M KNO_3 and isolated from aqueous solution by addition of NH_4PF_6, extraction of $[Ru(vbpy)_2((EtCO_2)_2bpy)](PF_6)_2$ into CH_2Cl_2, and rotary evaporation of CH_2Cl_2. The dark orange solid was further purified by column chromatography on alumina eluting with 2:1 toluene−acetonitrile.

Anal. Calcd for $C_{42}H_{40}F_{12}N_6O_4P_6Ru$: C, 46.54; N, 7.75; H, 3.72. Found: C, 44.82; N, 7.44; H, 3.76.

The ethyl ester complex was hydrolyzed to the dicarboxylic acid by dissolving ~0.15 g of complex in 30 mL methanol and adding 2 mL of water and 0.5 mL of 50% v/v NaOH. The solution was stirred for 2 h. The diacid complex $[Ru(vbpy)_2((CO_2H)_2bpy)](PF_6)_2$ was precipitated by dropwise addition of HPF_6 until the solution was acidic. The precipitate was collected, washed with water and diethyl ether, and dried in vacuo overnight.

Preparation of $[Ru(vbpy)_2(dppe)](PF_6)_2$ (dppe = *cis*-1,2-Bis-(diphenylphosphino)ethylene). $[Ru(vbpy)_2(dppe)](PF_6)_2$ was prepared in a manner similar to that for $[Ru(vbpy)_2(dcb)](PF_6)_2$. Briefly, a reaction mixture of $Ru(vbpy)_2Cl_2 \cdot 2H_2O$ (1 equiv), dppe (2.2 equiv), and hydroquinone (4 equiv) was combined in a solution of 2:1 $CH_3CH_2OH-H_2O$, and the mixture was deaerated by bubbling with Ar for 15 min. The reaction was heated to reflux under Ar for 3 h in the dark during which the color of the solution turned from deep purple to pale orange. The solution was allowed to cool for 1 h and then the ethanol evaporated under vacuum. The remaining aqueous solution was diluted with 1.5 L of H_2O and loaded onto a 12 in. SP Sephadex C-25 cationic exchange column. The product was eluted with 0.2 M NaCl as a tight yellow band. The addition of NH_4PF_6 resulted in the precipitation of $[Ru(vbpy)_2(dppe)](PF_6)_2$ from water. This product was extracted into CH_2Cl_2, evaporated to dryness, and dissolved in a minimum amount of CH_3CN. The final product was precipitated into ether and dried in air.

^1H NMR (CD_3CN, 20 °C): δ 2.28 (s, 3H), 2.48 (s, 3H), 5.69 (dd, 2H), 6.18 (dd, 2H), 6.40−7.76 (m, 32H), 8.05 (dd, 2H), 8.60 (m, 2H).

Anal. Calcd for $C_{52}H_{46}F_{12}N_4P_4Ru \cdot H_2O$: C, 52.08; N, 4.67; H, 4.04; P, 10.34. Found: C, 52.19; N, 4.60; H, 4.10; P, 10.31.

Measurements. Electrochemical measurements were performed with either a PAR 263 or PAR 273 potentiostat interfaced to a PC with data acquisition software written in-house. Electropolymerization was carried out in a two-compartment cell with the reference electrode separated from the working and counter electrodes by a fine frit and the Pt gauze counter electrode held parallel to the working electrode surface. Cyclic voltammetry (CV) was carried out in a three-compartment H-cell with a coiled Pt wire counter electrode. A Ag/0.01 M $AgNO_3$ in 0.1 M TBAH/CH_3CN reference electrode was used, and its potential was determined relative to SSCE by measuring the open circuit potential between the two electrodes. All potentials are uncorrected for junction potentials and are reported versus SSCE.

Absorption spectra of derivatized TiO_2 electrodes were obtained in air on an HP 8451A diode-array spectrometer. Spectra were distorted by the large TiO_2 absorption which tails into the visible, and variations in TiO_2 film thickness between samples make background correction difficult. To minimize these distortions, the absorbance spectrum of an underivatized TiO_2 electrode was subtracted from the spectrum of each sample, and the resulting spectrum was normalized to zero absorbance in the flat background region from 700 to 800 nm. Light-harvesting efficiency (LHE), the percent light absorbed by the chromophores, was calculated for each film from the absorbance spectra as $LHE = (1 - 10^{-abs})$.

Luminescence spectra were recorded on a Spex Fluorolog-2 emission spectrometer equipped with a 450 W Xe lamp and a cooled 10-stage Hamamatsu R928 photomultiplier. Spectra were collected with 470 nm excitation in a front face geometry with TiO_2 electrodes placed in a glass cuvette containing CH_3CN.

Photocurrent measurements were carried out in a thin-layer, two electrode cell. The counter electrode was a Pt foil sealed in a block of epoxide resin (Buehler) to form the cell base. The TiO_2 electrode was sandwiched against the counter electrode with a 0.1 mm Teflon spacer, and a 0.5 M NaI and 0.05 M I_2 in propylene carbonate solution was drawn into the cell by capillary action. The irradiation source was a 75 W xenon lamp powered by a high precision constant current source coupled to a f4-matched monochromator with 1200 lines/in. gratings. The light from the monochromator was passed through two glass lenses and onto either a calibrated detector (UDT Instruments, model S370 optometer) or Si photodiode calibrated with the UDT detector for light intensity measurement or the thin-layer TiO_2 photoelectrochemical cell for photocurrent measurement. Incident photon to current conversion efficiency (IPCE) at each incident radiation wavelength was calculated as

$$\mathrm{IPCE}\ (\lambda) = \frac{(1240\ \mathrm{eV\ nm})I_{ph}}{\lambda P_0}$$

where I_{ph} is the photocurrent density in μA cm^{-2}, λ is the wavelength of incident radiation in nm, and P_0 is the photon flux in mW cm^{-2}. The absorbed photon to current conversion efficiency (APCE) was calculated by dividing the IPCE by LHE at each λ.

Surface Attachment and Electropolymerization. The electrodes were derivatized with $[Ru(vbpy)_2(dcb)](PF_6)_2$ (**1**$(PF_6)_2$) or $[(bpy)_2(CN)Ru(CN)Ru(dcb)_2(NC)Ru(CN)(bpy)_2](PF_6)_2$ (**2**$(PF_6)_2$) by soaking for 24−72 h in ethanol or acetonitrile solutions containing ~1 mM of the complex. Immediately prior to introduction to the dye solution, electrodes were heated to 400 °C under O_2 for 15 min to remove adsorbed water. The electrodes were cooled to ~80 °C and placed in the dye solution while still warm.

Polymer-modified TiO_2 photoanodes were prepared by reductive electropolymerization of $[Ru(vbpy)_3](PF_6)_2$, $[Zn(vbpy)_3](PF_6)_2$, or $[Ru(vbpy)_2(dppe)](PF_6)_2$ on electrodes derivatized by adsorption of $[Ru(vbpy)_2(dcb)](PF_6)_2$. Electrodes with adsorbed **1**$(PF_6)_2$ were placed in a two compartment cell with a platinum gauze counter electrode positioned parallel to the TiO_2 film and cycled reductively past the vbpy ligand reduction potentials in acetonitrile containing 0.1 M TBAH and 0.5 mM $[Ru(vbpy)_3](PF_6)_2$, $[Zn(vbpy)_3](PF_6)_2$, or $[Ru(vbpy)_2(dppe)](PF_6)_2$. Between 3 and 100 reductive cycles were used to obtain a range of polymer surface coverages. For some

(22) Meyer, T. J.; Sullivan, B. P.; Caspar, J. V. *Inorg. Chem.* **1987**, *26*, 4145.
(23) Moss, J. A. Ph.D., University of North Carolina at Chapel Hill, 1997.
(24) Sullivan, B. P.; Salmon, D. J.; Meyer, T. J. *Inorg. Chem.* **1978**, *17*, 3334.

samples, the ITO was masked with Apiezon wax to expose only the TiO_2-coated area to the polymerization solution. Differences in films produced on masked and unmasked electrodes were not noticeable with the exception that only unmasked areas of ITO exposed to solution were coated with polymer during the polymerization.

Films of poly-$[Ru(vbpy)_3]^{2+}$ on TiO_2 were prepared in the same way but with no surface-adsorbed complex. An identical procedure was followed to prepare electrodes modified with poly-Ru(CN)-Ru(NC)Ru^{2+} except that an electrode derivatized with surface adsorbed **2**$(PF_6)_2$ was cycled in acetonitrile containing 0.1 M TBAH and 0.5 mM **2**$(PF_6)_2$.

AFM and XPS Surface Characterization. The surface structures of several derivatized TiO_2 electrodes were investigated by using tapping mode atomic force microscopy (TM-AFM). The measurements were conducted under ambient conditions with a Nanoscope III from Digital Instruments and silicon cantilevers with a resonance frequency of ~300 kHz (Digital Instruments). The images were flattened and plane fitted prior to analysis. The root-mean-square (rms) roughness was calculated by software provided by the manufacturer.

Depth profiles were obtained by X-ray photoelectron spectroscopy by using a Perkin-Elmer Physical Electronics model 5400 spectrometer. A differentially pumped Ar^+ ion gun (4 kV, 25 mA emission current) was used to sputter the film surface, and a Mg Kα X-ray source (400 W, 15 kV) irradiated the exposed surface during 2-min sputter intervals. The sputtered area was approximately 10 mm^2, and the analyzed area was 0.95 mm^2. The hemispherical analyzer pass energy was 35.75 eV, and the angle of collection was 45°. Quantitative atomic ratios were calculated by using the instrumental relative sensitivity factors and integrated photoelectron peak areas.

Results

Dye Adsorption. There is a well-developed chemistry of surface modification of TiO_2 with salts such as $[Ru(dcb)_3](PF_6)_2$ which contain carboxylic acid functionalities on one or more bipyridyl ligands. The vbpy derivative $[Ru(vbpy)_2(dcb)](PF_6)_2$ adsorbs to 8−12 μm thick films of TiO_2 on ITO from CH_3CN or CH_3CH_2OH solutions, resulting in highly absorbing films with OD ~ 1.2−1.8 at the metal-to-ligand charge transfer (MLCT) maximum at 467 nm. On the basis of an extinction coefficient $\epsilon = 13\,000\ cm^{-1}\ M^{-1}$, the surface coverage Γ was calculated to be from 9.2×10^{-8} to 13.8×10^{-8} mol cm^{-1}. The cyano-bridged salt [Ru(CN)Ru(NC)-Ru]$(PF_6)_2$ also adsorbs on nanocrystalline TiO_2 films at a level ~50% that of $[Ru(vbpy)_2(dcb)](PF_6)_2$, on the basis of a per molecule comparison as shown by absorbance measurements. On a per Ru basis, the cyano-bridged complex provides a ~50% greater coverage.

Electropolymerization. Reductive cycling of ITO/TiO_2 electrodes from −0.3 to −1.7 V with and without adsorbed **1**$(PF_6)_2$ in solutions containing $[Ru(vbpy)_3](PF_6)_2$, $[Zn(vbpy)_3](PF_6)_2$, or $[Ru(vbpy)_2(dppe)](PF_6)_2$ results in the formation of thin electropolymerized films as evidenced by the increase in peak current for vbpy reduction upon successive reduction cycles (Figure 1) and UV−visible monitoring (Figure 2). The vbpy reductive waves are obscured by the large background current due to charging of the TiO_2 at an onset potential of ~−0.7 V. For films of

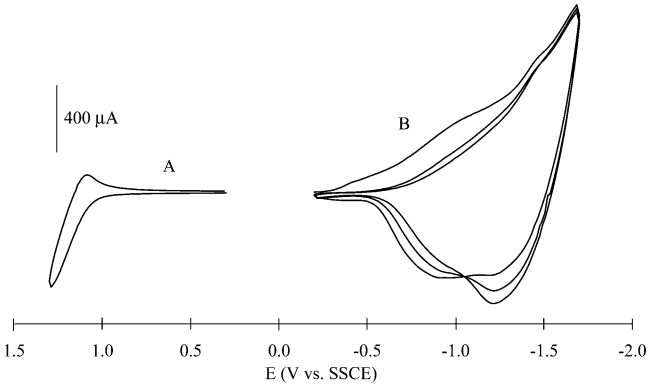

Figure 1. (A) Oxidative sweep at 100 mV/s of a TiO_2/ITO electrode in CH_3CN 0.5 mM in $[Ru(vbpy)_3](PF_6)_2$ and 0.1 M in TBAH followed by (B) three reductive electropolymerization sweeps at ITO/TiO_2 at 100 mV/s.

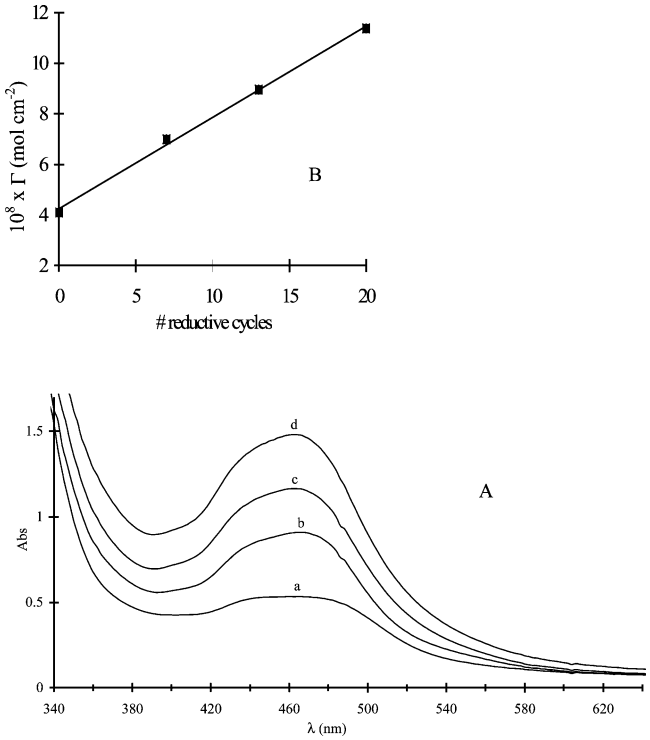

Figure 2. (A) UV−visible absorption spectra of of poly-$[Ru(vbpy)_3](PF_6)_2$ during electropolymerization on a ITO/TiO_2 electrode with adsorbed $[Ru(vbpy)_2(dcb)](PF_6)_2$ before polymerization (a) and after 7 (b), 13 (c), and 20 (d) cycles from −0.4 to −1.7 V in CH_3CN 0.5 mM in $[Ru(vbpy)_3](PF_6)_2$ and 0.1 M in TBAH. (B) Plot of Γ_{pol} versus number of reductive cycles.

$[Ru(vbpy)_3](PF_6)_2$, the amount of complex incorporated in the film can be monitored by the increase in absorbance of the film at 460 nm. The polymer surface coverage, Γ_{pol} (mol cm^{-2}), calculated by assuming $\epsilon = 13\,000\ cm^{-1}\ M^{-1}$ at 458 nm,[2] is proportional to the concentration of $[Ru(vbpy)_3](PF_6)_2$ in the external solution and the number of reductive cycles as shown in Figure 2. Similarly, reductive cycles at ITO/TiO_2 electrodes derivatized with adsorbed **2**$(PF_6)_2$ in CH_3CN solutions 0.5 mM in **2**$(PF_6)_2$ and 0.1 M in TBAH result in polymer films with a total surface coverage ~2× that of the adsorbed trimer. The coverage for films of $[Zn(vbpy)_3](PF_6)_2$ was estimated from the number of reductive cycles and growth of vbpy reductive waves as compared to those

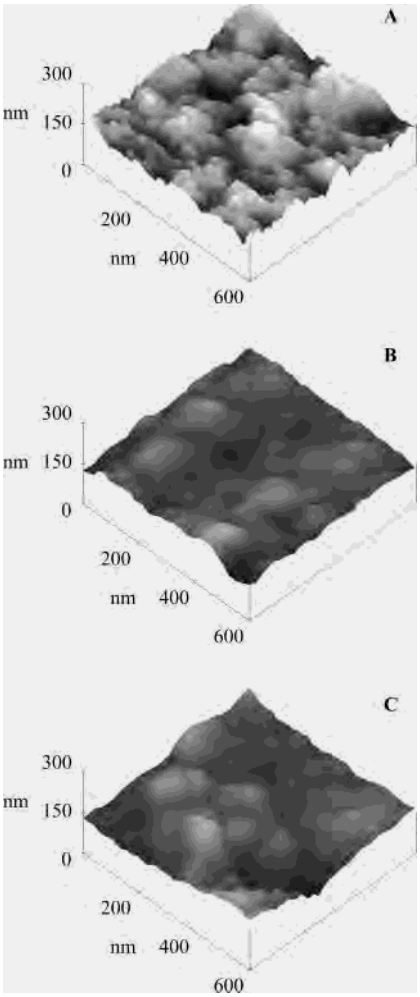

Figure 3. AFM surface images. Details are in the text.

of $[Ru(vbpy)_3](PF_6)_2$. For $[Ru(vbpy)_2(dppe)](PF_6)_2$, the coverage was determined by UV−vis measurement at 380 nm by using $\epsilon = 14\,000\ cm^{-1}\ M^{-1}$.

Surface Characterization. Tapping mode AFM was used to study the topography of TiO_2 electrodes before and after electropolymerization. The AFM image of a TiO_2 film with only adsorbed **1**$(PF_6)_2$ (Figure 3A) illustrates the porous and particulate nature of the films and the presence of small TiO_2 particle aggregates. The root-mean-square (rms) roughness of the surface illustrated was 17.8 nm. Images of TiO_2 with adsorbed-$[Ru(vbpy)_2(dcb)](PF_6)_2$/poly-$[Zn(vbpy)_3](PF_6)_2$ and ads-$[Ru(vbpy)_2(dcb)](PF_6)_2$/poly-$[Ru(vbpy)_3](PF_6)_2$ are shown in Figure 2B,C. The surface roughness factors for both were smaller, 10.72 and 12.09 nm, respectively. TM-AFM images were not able to resolve the adsorbed **1**$(PF_6)_2$ on TiO_2 particles because of the tip size (5−10 nm), but they do reveal that significant changes occur after electropolymerization with features as large as 200 nm appearing on these surfaces. Compared to the textured surfaces of agglomerates of small TiO_2 particles before polymerization, the surfaces of these large features are much smoother. This suggests polymerization partially fills in the features defining the surface roughness.

X-ray photoelectron spectroscopy (XPS) coupled with Ar^+ sputtering measurements was used to investigate the spatial distribution of polymers within the TiO_2 matrix. Depth profiling was conducted on a TiO_2 film with ads-$[Ru(vbpy)_2(dcb)](PF_6)_2$/poly-$[Zn(vbpy)_3](PF_6)_2$. The Ru and Zn concentrations were ratioed to Ti. Over a total sputter time of 60 min the ∼1:1 Zn/Ti and ∼1:2 Ru/Ti ratios were maintained demonstrating a fairly homogeneous profile from the surface to 0.4 μm into the TiO_2 film structure.

Photoelectrochemical Measurements. In Figure 4 are shown photocurrent action spectra for TiO_2 films with adsorbed **1**$(PF_6)_2$, ads-$[Ru(vbpy)_2(dcb)](PF_6)_2$/poly-$[Ru(vbpy)_3](PF_6)_2$, ads-$[Ru(vbpy)_2(dcb)](PF_6)_2$/poly-$[Zn(vbpy)_3](PF_6)_2$, and ads-$[Ru(vbpy)_2(dcb)](PF_6)_2$/poly-$[Ru(vbpy)_2$-

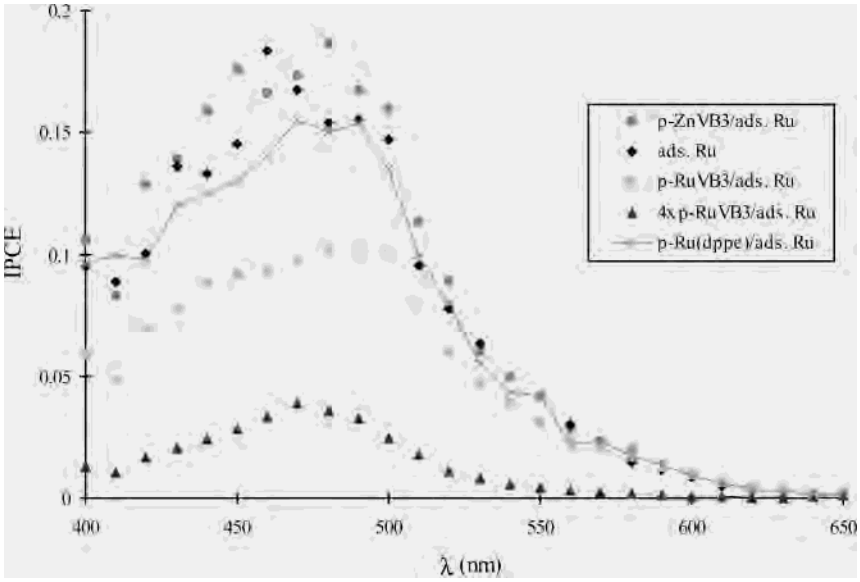

Figure 4. Photocurrent action spectra for TiO_2 electrodes derivatized with adsorbed $[Ru(vbpy)_2(dcb)](PF_6)_2$ (◆), ads-$[Ru(vbpy)_2(dcb)](PF_6)_2$/∼$1.2 \times 10^{-8}$ mol cm^{-2} poly-$[Zn(vbpy)_3](PF_6)_2$ (●), ads-$[Ru(vbpy)_2(dcb)](PF_6)_2$/$1.2 \times 10^{-8}$ mol cm^{-2} poly-$[Ru(vbpy)_2(dppe)](PF_6)_2$ (×), adsorbed $[Ru(vbpy)_2(dcb)](PF_6)_2$/$1.2 \times 10^{-8}$ mol cm^{-2} poly-$[Ru(vbpy)_3](PF_6)_2$ (■), and adsorbed $[Ru(vbpy)_2(dcb)](PF_6)_2$/$4.4 \times 10^{-8}$ mol cm^{-2} poly-$[Ru(vbpy)_3](PF_6)_2$ (▲). Spectra were acquired in propylene carbonate containing 0.5 M NaI and 0.05 M I_2.

Table 1. Summary of Dye Stability of Adsorbed and Electropolymerized Films on ITO/TiO_2 Electrodes in Aqueous Solutions

dyes					
ads complex	electropolymerized complex	no. of polym cycles	$10^8\Gamma_{pol}$[a] (mol cm^{-2})	pH[b]	dye loss (soaking time)
	$[Ru(vbpy)_3]^{2+}$	31	1.1	1−14	no loss (3 wk)
$[Ru(vbpy)_2(dcb)]^{2+}$		0	0	2	42% (30 min)
				9	75% (30 min)
				14	100% (10 min)
$[Ru(vbpy)_2(dcb)]^{2+}$	$[Ru(vbpy)_3]^{2+}$	70	7.3	1−14	no loss (3 wk)
		42	4.4	1−14	no loss (3 wk)
		31	1.2	1−14	no loss (3 wk)
		9	0.6	1	90% loss (30 min and 3 wk)
$[Ru(vbpy)_2(dcb)]^{2+}$	$[Zn(vbpy)_3]^{2+}$	42	∼4.4[c]	7	85% loss (10 min and 3 wk)
		31	∼1.2[c]	7	86% loss (10 min and 3 wk)
		6	∼0.3[c]	7	90% (1 wk and 3 wk)
$[Ru(vbpy)_2(dcb)]^{2+}$	$[Ru(vbpy)_2(dppe)]^{2+}$	50	2.1[d]	1−14	no loss (3 wk)
		31	0.8[d]	7	80% loss (30 min and 3 wk)
		9	0.2[d]	1	90% (30 min and 3 wk)

[a] Surface coverage of polymer, Γ_{pol}, calculated from the difference in absorbance before and after electropolymerization using $\Delta abs = 1000\epsilon\Gamma$, with ϵ = 13 000 cm^{-1} M^{-1} at 458 nm. [b] Solutions are 0.1 M $HClO_4$ (pH = 1), phosphate buffer (pH = 7), and 0.1 M NaOH (pH = 14). [c] Surface coverages were estimated by comparison to films of ads-$[Ru(vbpy)_2(dcb)](PF_6)_2$/poly-$[Ru(vbpy)_3](PF_6)_2$ prepared under identical conditions. [d] Surface coverage calculated from $\Delta abs = 1000\epsilon\Gamma$ with ϵ = 14 000 cm^{-1} M^{-1} at 380 nm.

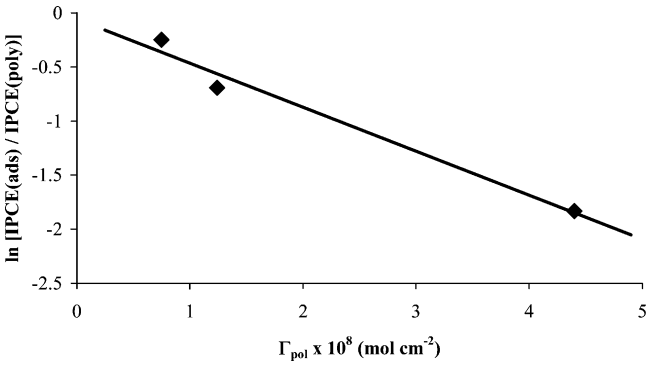

Figure 5. Logarithmic fit of IPCE (see text) versus electropolymerized surface coverage, Γ_{pol}, for TiO_2 films with ads-$[Ru(vbpy)_2(dcb)](PF_6)_2$/poly-$[Ru(vbpy)_3](PF_6)_2$. Measurements were made in propylene carbonate with 0.5 M NaI and 0.05 M I_2.

$(dppe)](PF_6)_2$ in propylene carbonate containing 0.1 M NaI and 0.05 M I_2. The photocurrents for TiO_2 with ads-$[Ru(vbpy)_2(dcb)](PF_6)_2$ and ads-$[Ru(vbpy)_2(dcb)](PF_6)_2$/poly-$[Zn(vbpy)_3](PF_6)_2$ are noticeably larger (IPCE = 0.18) than for TiO_2|ads-$[Ru(vbpy)_2(dcb)](PF_6)_2$/poly-$[Ru(vbpy)_3](PF_6)_2$ (IPCE = 0.10 and 0.03). They are comparable to photocurrents observed for ads-$[Ru(vbpy)_2(dcb)](PF_6)_2$/poly-$[Ru(vbpy)_2(dppe)](PF_6)_2$ (IPCE = 0.16). Films of poly-$[Ru(vbpy)_3](PF_6)_2$ with no adsorbed underlayer exhibit photocurrents lower by a factor of 5. An increase (4×) in the amount of electropolymerized poly-$[Ru(vbpy)_3](PF_6)_2$ results in a more than 2-fold decrease in the IPCE for the ads-$[Ru(vbpy)_2(dcb)](PF_6)_2$/poly-$[Ru(vbpy)_3](PF_6)_2$ film. As shown by the data in Figure 5, there is a logarithmic decrease in the ratio ln [IPCE(ads)/IPCE(poly)] with an increasing poly-$[Ru(vbpy)_3](PF_6)_2$ surface coverage. The slope is -3.8×10^9 (mol cm^{-2})$^{-1}$.

Signicantly, the decrease in IPCE with increasing electropolymerized polymer thickness was not observed for $[Ru(CN)Ru(NC)Ru](PF_6)_2$ at least for thin monolayer coverages. Electropolymerization of **2**$(PF_6)_2$ by 5 reductive sweeps at 100 mV/s in CH_3CN 0.1 M in TBAH and 0.5 mM in **2**$(PF_6)_2$ results in a ∼2× increase in surface coverage over adsorbed **2**$(PF_6)_2$ as shown by UV−visible measurements. The additional sensitizer in this case increases the IPCE at 440 nm to a maximum value of 29% for ads-$[Ru(CN)Ru(NC)Ru](PF_6)_2$/poly-$[Ru(CN)Ru(NC)Ru](PF_6)_2$ compared to 22% for ads-**2**$(PF_6)_2$. Correcting for the difference in LHE due to greater surface coverage of $[Ru(CN)Ru(NC)Ru](PF_6)_2$ in the adsorbed/electropolymerized sample gives APCE (APCE = IPCE/LHE) values of 37% for both samples at 440 nm. Addition of more polymer by increasing the number of reductive sweeps in the electropolymerization eventually causes a decrease in IPCE for **2**$(PF_6)_2$-modified ITO/TiO_2 as for ads-$[Ru(vbpy)_2(dcb)](PF_6)_2$/poly-$[Ru(vbpy)_3](PF_6)_2$ films.

Surface Stability. The surface stabilities of films of ads-$[Ru(vbpy)_2(dcb)](PF_6)_2$, ads-$[Ru(vbpy)_2(dcb)](PF_6)_2$/poly-$[Ru(vbpy)_3](PF_6)_2$, ads-$[Ru(vbpy)_2(dcb)](PF_6)_2$/poly-$[Zn(vbpy)_3](PF_6)_2$, and ads-$[Ru(vbpy)_2(dcb)](PF_6)_2$/poly-$[Ru(vbpy)_2(dppe)](PF_6)_2$ were investigated in acetonitrile and water. In acetonitrile, the visible absorption spectra of all four films were unchanged after 2 weeks of soaking. For films with ads-$[Ru(vbpy)_2(dcb)](PF_6)_2$, a small (5−10%) loss of dye was observed following photocurrent measurements, presumably due to desorption into the propylene carbonate/NaI electrolyte solution. No loss from the ads/poly films was observed following photocurrent measurements in propylene carbonate.

The results of a series of aqueous solution stability studies are summarized in Table 1. For films of ads-$[Ru(vbpy)_2(dcb)](PF_6)_2$/poly-$[Ru(vbpy)_3](PF_6)_2$, ads-$[Ru(vbpy)_2(dcb)](PF_6)_2$/poly-$[Ru(vbpy)_2(dppe)](PF_6)_2$, and poly-$[Ru(vbpy)_3](PF_6)_2$, no loss of polymer or adsorbed complex was observed after soaking for up to 3 weeks in aqueous solutions from pH 1 to 14 in samples with electropolymerized surface coverages $>1.1 \times 10^{-8}$ mol cm^{-2}.

Lower surface coverages greatly decrease aqueous stability. Films of ads-$[Ru(vbpy)_2(dcb)](PF_6)_2$/poly-$[Zn(vbpy)_3](PF_6)_2$ are much less stable than films of poly-$[Ru(vbpy)_3](PF_6)_2$ under comparable conditions. Approximately 90% of the dye in these films was lost at pH 7 in 10 min although the remaining dye was not desorbed upon continued soaking

for at least 3 weeks. The instability of the Zn^{II} films results from the lability of Zn^{II} toward substitution; see below.

Discussion

The sensitization of nanocrystalline ITO/TiO_2 films with electropolymerized films and complex assemblies provides an increased level of sophistication in the structure and design of possible devices. The focus of this work was the use of polymer films for stabilization of internal dye layers, but there are possible extensions to catalysis,[25−27] multilayer effects,[28] and microfabrication[29−31] based on electropolymerized films which could conceivably be applied to these nanocrystalline electrodes.

Electropolymerization on ITO/TiO_2. The results of the investigations described here establish the basic characteristics of electropolymerized film behavior on ITO/TiO_2. The electropolymerization of poly-[$Ru(vbpy)_3$]$(PF_6)_2$ establishes that films do form on these surfaces. On the basis of the results of the depth resolution experiments, electropolymerization leads to film formation from the film−solution interface to a considerable distance into the film with a near constant composition. Electropolymerization appears to occur throughout the TiO_2 microporous films[32] rather than by electron-transfer initiation at the ITO/TiO_2 interface.

At oxidative potentials TiO_2 is an insulator. The appearance of the $Ru^{III/II}$ wave at the end of the electropolymerization cycle provides evidence that the films are in contact with the underlying ITO electrode. The mechanism of electron transfer is by $Ru^{III} \leftarrow Ru^{II}$ electron hopping from the ITO−TiO_2 interface through the electropolymerized film to the film−solution interface. A related mechanism has been identified for adsorbed complexes such as ads-**1**$(PF_6)_2$, where $Ru^{II} \rightarrow Ru^{III}$ oxidation occurs from the ITO−TiO_2 interface to the film−solution interface by cross-surface electron-transfer hopping.[32,33]

The formation of poly-[$Ru(vbpy)_3$]$(PF_6)_2$ on ITO/TiO_2 is accompanied by a linear increase in absorbance upon successive reductive scans. AFM surface images obtained from these modified surfaces, Figure 3, demonstrate that considerable change occurs in physical taxonomy from the rough texture of the initial TiO_2 particulate surface, after electropolymerizing with either [$Zn(vbpy)_3$]$(PF_6)_2$ or [$Ru(vbpy)_3$]$(PF_6)_2$. Electropolymerization is accompanied by a noticeable decrease in surface roughness, presumably due to the spatially unsymmetrical formation of a polymeric

Scheme 1

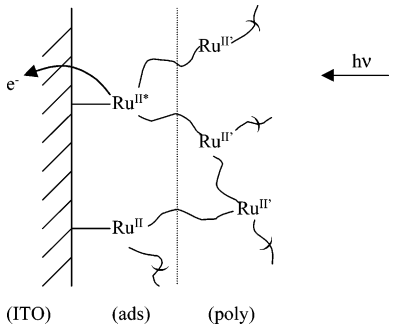

overlayer across the surface which masks some of the surface features. Increases in Ru^{II} surface coverage by continued electropolymerization can greatly increase absorbance and LHE for the electropolymerized films. However, the enhanced absorptivity is only of value for photocurrent production if the excitation of Ru^{II} sites remote from the TiO_2−film interface results in net injection of electrons into the TiO_2 conduction band. This can only occur if efficient energy or electron transfer occurs to complexes adsorbed to or near the surface which are electronically coupled to the surface. This is not the case for poly-[$Ru(vbpy)_3$]$(PF_6)_2$; see below.

The results of the electrochemical and spectral experiments demonstrate that it is possible to electropolymerize overlayers of poly-[$Ru(vbpy)_3$]$(PF_6)_2$, poly-[$Zn(vbpy)_3$]$(PF_6)_2$, and poly-[$Ru(vbpy)_2(dppe)$]$(PF_6)_2$ on ads-[$Ru(vbpy)_2(dcb)$]$(PF_6)_2$. As on the bare electrode, the extent of overlayer formation depends on the concentration of complex in the external solution and the number of reductive scans.

As illustrated below for "end-to-end" coupling, electropolymerization at the surface results in chemical linkages between complexes formed by radical coupling reactions. The existence of multiple vbpy ligands provides a basis for cross-linking. A schematic illustration of the resulting, stabilized structure is shown in Scheme 1.

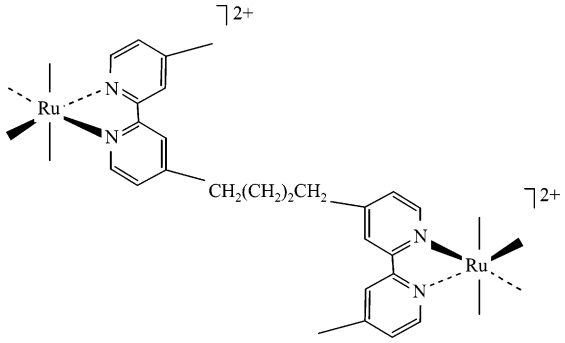

Aqueous Stability. The stabilities of films of ads-[$Ru(vbpy)_2(dcb)$]$(PF_6)_2$/poly-[$Ru(vbpy)_3$]$(PF_6)_2$ and ads-[$Ru(vbpy)_2(dcb)$]$(PF_6)_2$/poly-[$Ru(vbpy)_2(dppe)$]$(PF_6)_2$ are remarkable with no loss of complex as measured by absorbance measurements over the course of 3 weeks in aqueous solutions from pH 1 to pH 14. Films stabilized with an overlayer of poly-[$Zn(vbpy)_3$]$(PF_6)_2$ are unstable under the same conditions due to demetalation of the films. Zn^{2+} forms coordination complexes that are labile with regard to ligand exchange. In the electropolymerized films, the metal acts as

(25) Guadalupe, A. R.; Chen, X.; Sullivan, B. P.; Meyer, T. J. *Inorg. Chem.* **1993**, *32*, 5502.
(26) Murray, R. W.; Ewing, A. G.; Durst, R. A. *Anal. Chem.* **1987**, *59*, 379A.
(27) Abruna, H. D. *Coord. Chem. Rev.* **1988**, *86*, 135.
(28) Denisevich, P.; Abruna, H. D.; Leidner, C. R.; Meyer, T. J.; Murray, R. W. *Inorg. Chem.* **1982**, *21*, 2153.
(29) Gould, S.; Gray, K. H.; Linton, R. W.; Meyer, T. J. *Inorg. Chem.* **1992**, *31*, 5521.
(30) O'Toole, T. R.; Sullivan, B. P.; Meyer, T. J. *J. Am. Chem. Soc.* **1989**, *111*, 5699.
(31) Gould, S.; O'Toole, T. R.; Meyer, T. J. *J. Am. Chem. Soc.* **1990**, *112*, 9490.
(32) Trammell, S. A.; Meyer, T. J. *J. Phys. Chem. B* **1999**, *103*, 104.
(33) Stipkala, J. M.; Castellano, F. N.; Heimer, T. A.; Kelly, C. A.; Livi, K. J. T.; Meyer, G. J. *Chem. Mater.* **1997**, *9*, 2341.

a cross-linker holding together the electropolymerized strands. As illustrated below, loss of Zn^{2+} from the films results in the breakdown of the cross-linked structure and dissolution of the isolated fragments:[20]

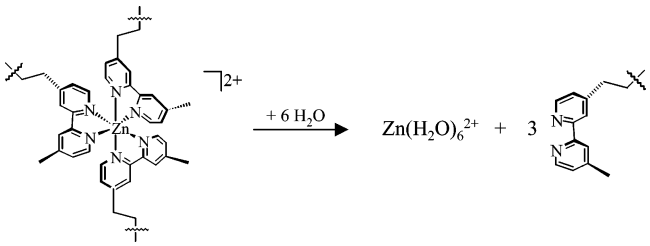

By contrast, surface structures overlaid with poly-[Ru(vbpy)$_3$](PF$_6$)$_2$ or poly-[Ru(vbpy)$_2$(dppe)](PF$_6$)$_2$ are stable. In these cases the Ru^{II} complexes are substitutionally inert and the cross-linking imparted by the metal complex remains intact.

As can be seen from the data in Table 1, stabilization of the surface-adsorbed dye molecules by electropolymerization of an overlayer depends on the extent of surface coverage. With ads-[Ru(vbpy)$_2$(dcb)](PF$_6$)$_2$ overlaid with limited poly-[Ru(vbpy)$_3$](PF$_6$)$_2$ there is significant loss of the adsorbed complex, but the loss occurs on a relatively short time scale with the remainder stabilized indefinitely. Presumably, surface stabilization by overlayer formation occurs by vinyl interlinking between adsorbed and overlayer molecules. This creates a local patchwork structure of vinyl-connected, insoluble clusters.

IPCE Characteristics: Design of Water-Stable Interfaces. As noted in the Introduction, a primary goal of this work was to prepare water-stable, photoactive interfaces on TiO_2. We ultimately developed a successful strategy on the basis of electropolymerization of an overlayer of [Ru(vbpy)$_2$(dppe)](PF$_6$)$_2$ on adsorbed [Ru(vbpy)$_2$(dcb)](PF$_6$)$_2$. It is of interest to follow the sequence of experiments that ultimately led to the final result.

Comparison of IPCE values for films of ads-[Ru(vbpy)$_2$(dcb)](PF$_6$)$_2$ and ads-[Ru(vbpy)$_2$(dcb)](PF$_6$)$_2$/poly-[Ru(vbpy)$_3$](PF$_6$)$_2$ in propylene carbonate with I_3^-/I^- are revealing. They show that the overlayer electropolymerized films are less efficient at converting incident photons into electrical current than the simple adsorbed films even though the layered films are more strongly absorbing. The aqueous stability of the composite films points to the formation of interlayer cross-linking between the adsorbed and electropolymerized layers.

The decrease in IPCE for the ads/poly films suggests that the electropolymerized overlayer acts minimally as a light filter, absorbing photons but not contributing to electron injection. The light filter effect is consistent with the logarithmic fall off in IPCE with surface coverage as shown in Figure 5.

The outer, electropolymerized layer may additionally decrease the measured IPCE values by acting as an energy-transfer trap. As illustrated in Scheme 2, contributions to the IPCE from the adsorbed layer may be diminished by competitive energy transfer to the outer layer followed by

Scheme 2

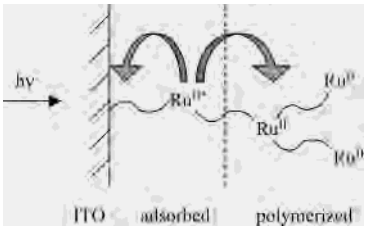

excited-state decay in the outer film. From emission measurements, $\Delta G^\circ \sim -0.1$ eV for energy transfer away from the electrode by the mechanism

$$\xrightarrow{h\nu} TiO_2-Ru^{II*}_{ads}-Ru^{II}_{poly} \rightarrow TiO_2-Ru^{II}_{ads}-Ru^{II*}_{poly}$$

The fact that IPCE values are comparable for ads-**1**(PF$_6$)$_2$ and ads-[Ru(vbpy)$_2$(dcb)](PF$_6$)$_2$/poly-[Zn(vbpy)$_3$](PF$_6$)$_2$ reinforces this conclusion. The poly-[Zn(vbpy)$_3$](PF$_6$)$_2$ overlayer is transparent in the visible region and has no low-lying excited states. The poly-[Zn(vbpy)$_3$](PF$_6$)$_2$ result also shows that electropolymerization does not contribute to the loss of IPCE solely by blocking the I_3^-/I^- couple from regenerating Ru^{II} by reduction of Ru^{III}. The charge types are the same, and the molecular dimensions of individual units in poly-[Zn(vbpy)$_3$](PF$_6$)$_2$ and poly-[Ru(vbpy)$_3$](PF$_6$)$_2$ are nearly the same.[22]

It is also revealing that electropolymerized films of poly-[Ru(vbpy)$_3$](PF$_6$)$_2$ without an ads-[Ru(vbpy)$_2$(dcb)](PF$_6$)$_2$ underlayer exhibit relatively low IPCE values. This shows that direct injection from the polymer film is also relatively inefficient. From an earlier study on the photophysical properties of Ru^{III}(vbpy$^{\bullet-}$) metal-to-ligand charge transfer (MLCT) excited states in poly-[Ru(vbpy)$_3$](PF$_6$)$_2$, there is a facile loss mechanism in the films that must compete successfully with photoinjection. The loss mechanism arises from low-energy trap sites in the electropolymerized films which are short-lived and populated by intrafilm energy transfer hopping.[34]

A contrasting behavior is observed for the IPCE characteristics of ads-[Ru(CN)Ru(NC)Ru](PF$_6$)$_2$/poly-[Ru(CN)Ru(NC)Ru](PF$_6$)$_2$ compared to ads-[Ru(CN)Ru(NC)Ru](PF$_6$)$_2$. Addition of an electropolymerized overlayer has no effect on the per photon absorbed current efficiency of the cell. IPCE values are the same within experimental error for films with and without a polymer overlayer. This points to efficient energy transfer to ads-[Ru(CN)Ru(NC)Ru](PF$_6$)$_2$ and unperturbed photoinjection following excitation at poly-**2**(PF$_6$)$_2$.

Overlayer electropolymerization of the organodiphosphine complex [Ru(vbpy)$_2$(dppe)]$^{2+}$ on ads-[Ru(vbpy)$_2$(dcb)](PF$_6$)$_2$ combined the stability of the ads-[Ru(vbpy)$_2$(dcb)](PF$_6$)$_2$/poly-[Ru(vbpy)$_3$](PF$_6$)$_2$ composite with the outer layer visible transparency of the analogous [Zn(vbpy)$_3$](PF$_6$)$_2$ composite. IPCE values were obtained in propylene carbonate with I_3^-/I^- comparable to those for ads-[Ru(vbpy)$_2$(dcb)](PF$_6$)$_2$.

The greatly decreased visible light absorptivity by the complex in the outer layer of the composite is a consequence

(34) Devenney, M.; Worl, L. A.; Gould, S.; Guadalupe, A.; Sullivan, B. P.; Caspar, J. V.; Leasure, R. M.; Gardener, J. R.; Meyer, T. J. *J. Phys. Chem. A* **1997**, *101*, 4535.

of the dppe ligand. It undergoes a significant d$\pi \rightarrow$ dppe back-bonding interaction with the metal which stabilizes the dπ levels and increases the d$\pi-\pi^*$ (bpy) energy gap. This shifts the lowest energy metal-to-ligand charge transfer (MLCT) bands to the low-energy ultraviolet. The complex is coordinatively stable to ligand loss which explains the stabilization by electropolymerized overlayers.

Preliminary photocurrent measurements were conducted in water on ads-$[Ru(vbpy)_2(dcb)](PF_6)_2$/poly-$[Ru(vbpy)_2(dppe)](PF_6)_2$ with the quinone/hydroquinone couple as the redox carrier. Initial data with hydroquinone at 0.1 M in water resulted in a significant photocurrent response. IPCE values were obtained which were ~50% of those obtained for I_3^-/I^- in propylene carbonate. It is also notable that the IPCE values were stable after 1 day of continuous measurement.

Acknowledgments are made to the Office of Basic Energy Sciences, U.S. Department of Energy, under Grant No. DE-FG02-96ER14607 for support of this research.

IC030081A